Polymer Chemistry

ROYAL SOCIETY OF CHEMISTRY

COMMUNICATION

View Article Online
View Journal | View Issue

Cite this: *Polym. Chem.*, 2022, **13**, 6114

Received 9th September 2022,
Accepted 9th October 2022

DOI: 10.1039/d2py01166b

rsc.li/polymers

Photomediated RAFT step-growth polymerization with maleimide monomers†

Samantha Marie Clouthier, Joji Tanaka * and Wei You *

Photomediated RAFT step-growth polymerization was performed with and without the presence of a photocatalyst using a trithiocarbonate-based CTA and a maleimide monomer. Under catalyst-free conditions, the polymerization proceeded with an appreciable rate under irradiation with blue and green light, which was extended to red light in the presence of ZnTPP.

Reversible addition fragmentation chain transfer (RAFT) polymerization, mediated by RAFT agents or chain transfer agents (CTAs) that seed and control the polymerization *via* chain transfer of the thiocarbonylthiol group, is generally considered as one of the most user friendly and versatile polymerization strategies.[1–3] Traditionally, RAFT polymerization has been driven by exogenous initiators; however, recent years have witnessed a rapid growth in the use of light to directly initiate RAFT polymerization.[4]

Depending on the chemical nature of the R/Z groups of the CTAs, the thiocarbonyl thiol group can directly absorb light of an appropriate wavelength to fragment into radicals to initiate the polymerization.[5] This intriguing photoinduced process was first described by Ostu and coworkers as initiation–chain transfer–terminator (iniferter) using UV irradiation.[6] Later, Zard *et al.* utilized this photoinduced fragmentation in organic synthesis for the insertion process before the invention of RAFT polymerization.[7] More recently, this process has been widely exploited using RAFT agents for polymerization under visible light (*i.e.*, RAFT-iniferter polymerization).[8–10]

In contrast to the RAFT-iniferter process, in which light directly fragments the CTA, another recently developed method relies on photoinduced energy/electron transfer (PET) *via* photocatalysts to indirectly fragment the CTA. While RAFT-iniferter typically requires high energy photons (*e.g.*, UV or blue), PET-RAFT allows versatility in wavelength selection and oxygen tolerance.[12–15] However, to date, most of the investigations into photomediated RAFT polymerization have been focused on controlled chain growth.

We recently reported a step-growth polymerization through the RAFT process by utilizing monomer and CTA pairs that selectively and efficiently yield single monomer unit inserted (SUMI) CTA adducts under stoichiometrically balanced conditions.[16] Moreover, we exploited commercially available bifunctional monomers, which were able to undergo RAFT step-growth polymerization, thereby increasing the accessibility of this new polymerization methodology.[17,18] However, the polymerizations in these reports were all driven by thermal decomposition of exogenous initiators at the cost of end group fidelity (Scheme 1A).

In general, high monomer conversion and high end-group fidelity are required to obtain a high molecular weight through the step-growth mechanism.[19] Therefore, using a photomediated strategy (*e.g.*, iniferter) that is rapid with limited loss of the end groups is especially desirable for RAFT step-growth polymerization. Moreover, Xu *et al.* demonstrated quantitative monomer conversion and SUMI-CTA adduct yield *via* PET-RAFT under balanced stoichiometric conditions.[20] Given these desirable features of the light-mediated RAFT polymerizations (iniferter and PET-RAFT), we set our goals to investigate both in our RAFT step-growth system. Importantly, given the different initiating mechanisms of iniferter and PET-RAFT, it would be interesting to compare the differences between these two light-mediated approaches in RAFT step-growth polymerization.

We first investigated RAFT-iniferter step-growth polymerization using three different wavelengths, red (λ_{max} = 625 nm), green (λ_{max} = 514 nm) and blue LED irradiation (λ_{max} = 458 nm), which overlap with visible light absorbance corresponding to the symmetry forbidden transition (n–π*) of the CTA (Fig. 1A).[21] In theory, photoactivation can occur from the end group CTA (activation pathway I, Scheme 1B) or from the backbone CTA (activation pathway II, Scheme 1B); each pathway would directly generate one of the two radical inter-

Department of Chemistry, University of North Carolina at Chapel Hill, Chapel Hill, NC, 27599-3290, USA. E-mail: joji@email.unc.edu, wyou@unc.edu

† Electronic supplementary information (ESI) available. See DOI: https://doi.org/10.1039/d2py01166b

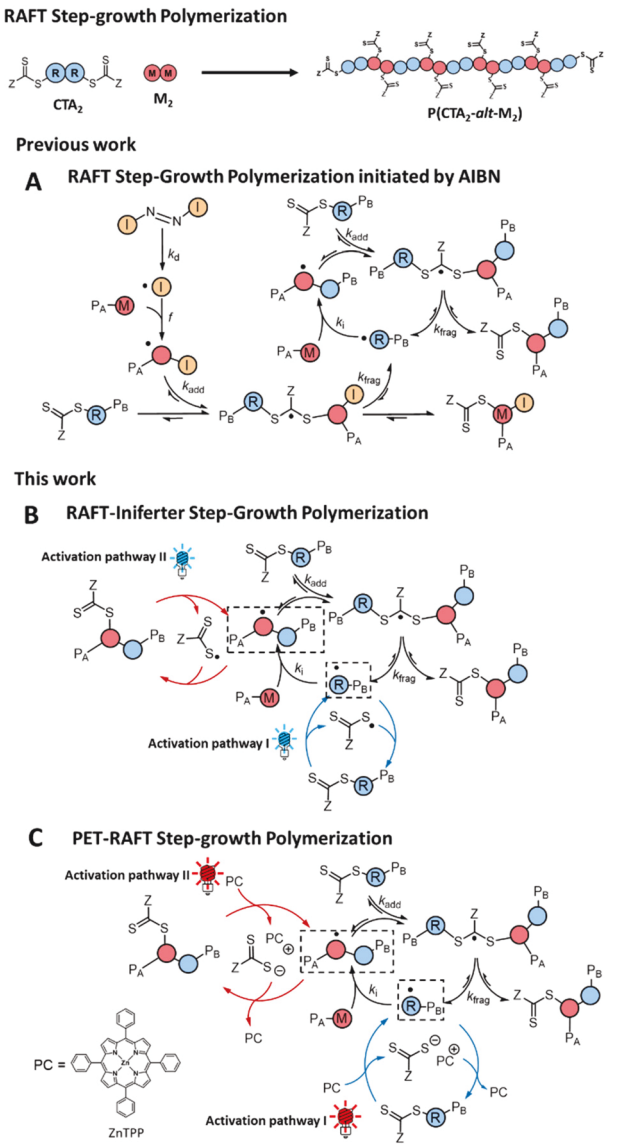

Scheme 1 Photo-mediated RAFT step-growth polymerization in this work.

mediates required for the RAFT step-growth cycle (dashed line, Scheme 1).

Experimentally, the reaction mixture was prepared as previously reported, using commercially available *N*,*N*′-(1,4-phenylene)dimaleimide as the bifunctional monomer (M_2) in tetrachloroethane (TCE), but without the addition of an exogenous initiator.[17] ^{1}H-NMR was used to determine monomer conversion as previously reported[17] and SEC analysis was used to determine the molecular weights relative to polystyrene standards in THF.

In our reaction setup (Fig. S1†), the polymerization proceeded rapidly during the initial 16 hours under blue and green light irradiation (p > 97%), though the molecular weight did not increase further beyond 16 hours (Tables S1–S3 and Fig. S2–S4†) despite the observation of a mild increase in monomer conversion (p > 98%). In contrast, under red light, the monomer conversion only reached 76% after 48 hours. The observed slower RAFT-iniferter SUMI kinetics with trithiocarbonates under red light was previously observed by others as well, despite the minimal overlap of the CTA with the red LED emission spectra.[22] Interestingly, the reaction kinetics significantly deviated from the linear trend in the semi-logarithmic plot with increasing conversion (Fig. 1B). This deviation from the first order kinetics can be explained by the blue shift in the n–π* absorbance of trithiocarbonate (Fig. 1A), as the end group CTA converts to the backbone CTA. Moad *et al.* reported that the n–π* absorbance of trithiocarbonates underwent a blue shift for less radically stabilized fragmentation;[23] in our case, the conversion of the ester-stabilised tertiary carbon radical fragmentation (*i.e.*, end group CTA) into maleimide secondary carbon radical fragmentation (*i.e.*, backbone CTA) would increase the energy requirement for the homolysis of the latter species, and thus the blue-shift as seen in Fig. 1A. We speculate that the preference for the photoinduced fragmentation of the end group CTA (activation pathway I, Scheme 1B) leads to deviation from the expected first order kinetics as the end group CTAs are consumed during the polymerization.

Nonetheless, the polymerization proceeded with step-growth molecular weight evolution under all wavelengths investigated, as indicated by the molecular weight averages (M_n, M_w and M_z) and conversion following the expected trend in accordance with Flory's equations.[11]

Utilising the RAFT-iniferter process to mediate RAFT step-growth polymerization was first reported by Zhu *et al.*[24] In their work, blue light was used to initiate the polymerization with xanthate-bearing ester-stabilized secondary carbon fragmentation as the CTA and vinyl ether as the monomer. Though successful step-growth molecular weight evolution was observed in their work, the molecular weight was limited (M_w = 4.2k) at high monomer conversion (p > 99%, $M_{w,th}$ = 57k).[24] In contrast, we obtained a higher molecular weight (M_w = 16k); however, it was still lower than expected at high monomer conversion (p = 98%, $M_{w,th}$ = 50k).

We next investigated PET-RAFT step-growth polymerization under the same reaction conditions (Scheme 1C). In comparison with RAFT-iniferter, PET-RAFT is known to have superior kinetics especially under irradiation of a longer wavelength.[22,25] We utilized ZnTPP as the photocatalyst in this study as it is affordable and widely used for trithiocarbonate-based CTAs (Fig. 2).[14] In addition, the UV-vis spectrum of ZnTPP reveals its Q-band absorbance that overlaps with those of the LEDs used for our study (Fig. 2A). In contrast to the iniferter-based approach, the photoactivation of the ZnTPP photocatalyst is speculated to result in a more stable thiocarbonyl anion *via* electron transfer (activation pathway I/II, Scheme 1C).[26–28] Though this charge transfer-based system has been reported to be optimum in polar solvents such as DMSO,[13,14] we found our dimaleimide monomer (M_2) to be insoluble in this solvent. In addition, we previously found DMSO to be an incompatible solvent for RAFT step-growth polymerization

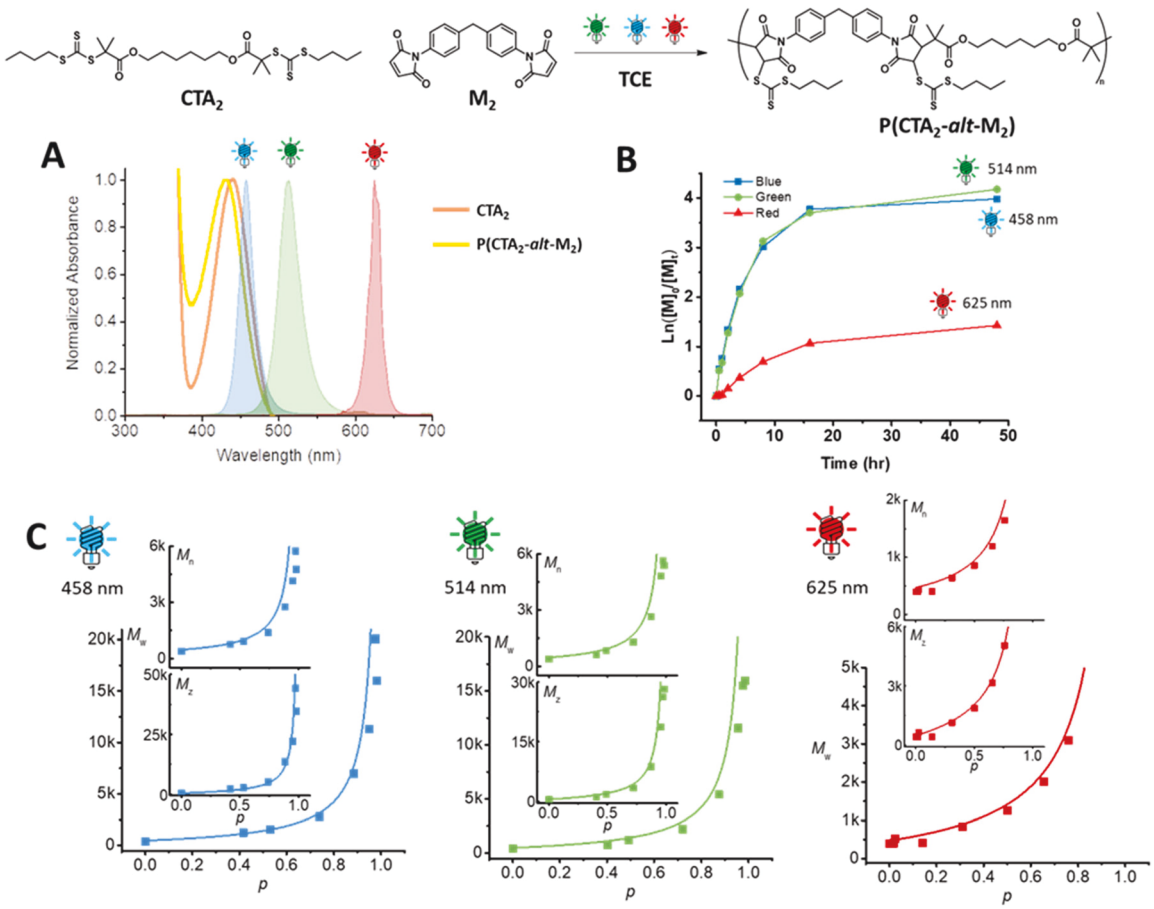

Fig. 1 A_2 + B_2 RAFT-iniferter step-growth polymerization. (A) Visible light absorption spectra of the bifunctional CTA, CTA_2 (orange line) and the resulting step-growth CTA backbone after polymerization (yellow line). The emission spectra from the LED light used in the photoreactor are plotted together. (B) Semi-logarithmic plot of polymerization kinetics under different light irradiation. (C) Evolution of the molecular weight averages (M_w, M_n, and M_z) from SEC analysis using polystyrene calibration, plotted together with monomer conversion (p) determined by ^{1}H NMR spectroscopy. These are plotted together with the theoretical line for step-growth molecular weight evolution that assumes no cyclization.[11]

using maleimide monomers.[16] Thus, we proceeded to use TCE as the solvent to favour the solubility of the monomer (M_2). Here, we used a molar ratio of CTA functionality to ZnTPP of 200 ($[CTA]_0/[ZnTPP]_0$ = 200) (Fig. S6–S8†). Interestingly, the initial rates were seemingly slower under blue and green light under PET-RAFT conditions when compared to catalyst free conditions (RAFT-iniferter); this observation contrasts to the comparison of kinetics in classical chain-growth systems where PET-RAFT is faster than RAFT-iniferter.[29] Nonetheless, the polymerization rate was significantly improved under red light irradiation in the presence of ZnTPP compared to catalyst-free conditions under the same irradiation (Fig. 2B). Interestingly, pseudo-first order kinetics with respect to monomer conversion was observed under blue, green and red light irradiation from the semi-logarithmic plot (Fig. 2B), indicating the number of reactive radical intermediates in the reaction cycle to remain constant, which is consistent with PET RAFT-SUMI kinetics reported in the literature.[25,30] In contrast to the catalyst-free conditions, the activation in PET-RAFT relies on the presence of a photocatalyst, which is the limiting reagent. Nonetheless, a slight deviation from the first order kinetics at high monomer conversion is still apparent, though to a lesser extent than that of iniferter. This observation suggests the rate-limiting generation of $R^{\bullet}$, which could also be attributed to the preference of selectivity for photoactivation of the end group CTA. It is noteworthy that though the initial rates were similar under all three wavelengths of light examined, the highest conversion (p = 99%) and molecular weight (M_w = 27k) were achieved under red light, suggesting possibly higher end-group fidelity. Nonetheless, under all three wavelengths, we found the polymerization to proceed through step-growth molecular weight evolution (Fig. 2C and Fig. S9†).

Though we anticipated the molecular weights obtained with the light-mediated RAFT step-growth polymerization to be higher than those of the thermal-initiated RAFT step-growth (since no exogenous initiator was used), we did not observe significant improvement in the molecular weight in the light-mediated cases. This observation could be possibly due to the difficulty in balancing the stoichiometry of the starting reagents or the presence of impurity in the commercial

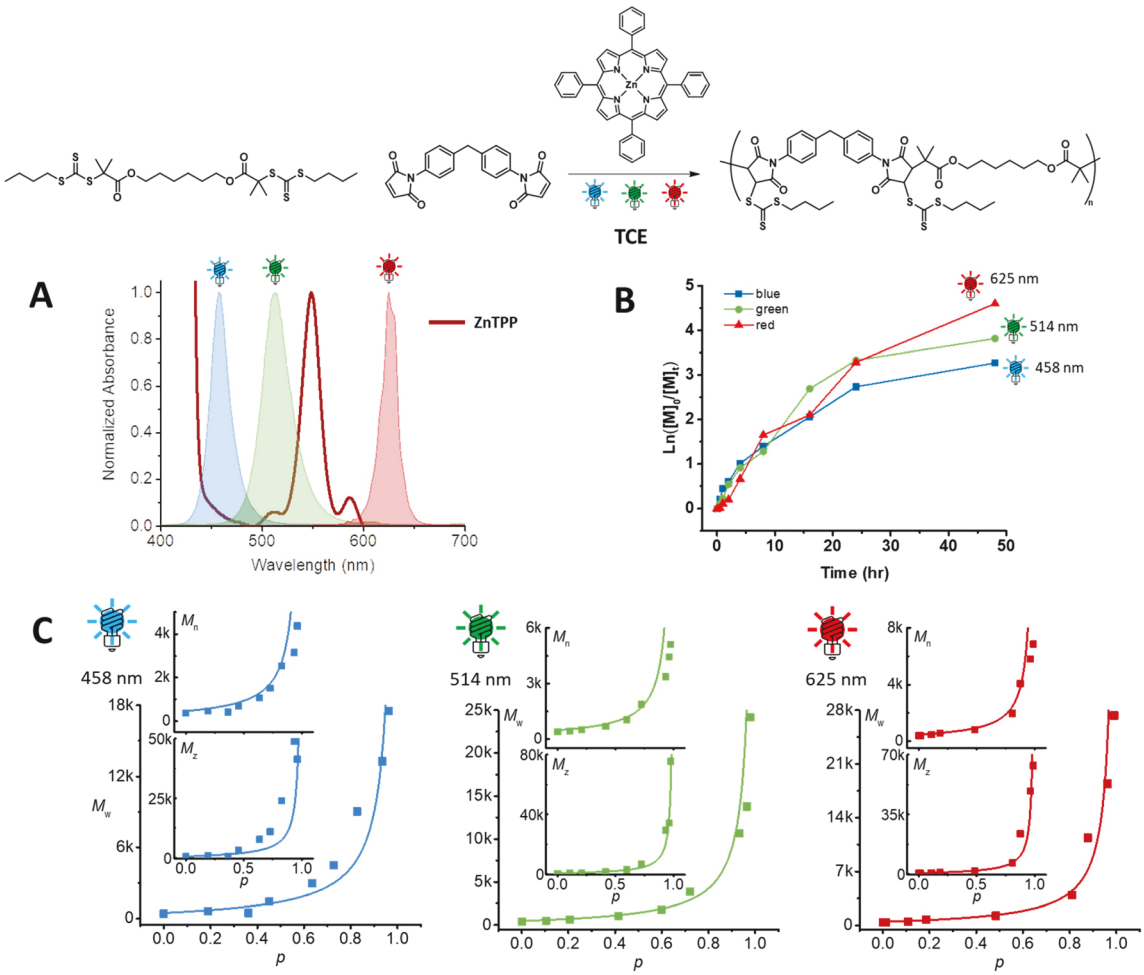

Fig. 2 A_2 + B_2 PET-RAFT step-growth polymerization. (A) The visible light absorption spectrum of the photocatalyst, ZnTPP (red line), plotted together with the emission spectra from the LED light used in the photoreactor. (B) Semi-logarithmic plot of polymerization kinetics under different light irradiation. (C) Evolution of the molecular weight averages (M_w, M_n, and M_z) from polystyrene calibration, plotted together with monomer conversion (p) determined by ^{1}H NMR spectroscopy. These are plotted together with the theoretical line for step-growth molecular weight evolution that assumes no cyclization.[11]

monomer. To explore the possible improvement in end-group fidelity with the photo-mediated system, we briefly examined PET-RAFT with an AB RAFT-step growth monomer (Table S7 and Fig. S10, S11†), which would ensure balanced stoichiometry. Interestingly, a difference between the theoretical M_w and the experimental value by a factor of 2 was observed ($M_{w,th}$ = 70k, M_w = 30k, Table S7†), which was consistent with our previous report when considering initiator-derived imbalanced stoichiometry.[16] We speculate that this difference is due to the large weight fraction of the lower molecular weight cyclic species formed during the polymerization, which inherently occurs more in the AB step-growth system.[31] Nevertheless, theoretical M_z follows more closely to the expected values as lower molecular weight species are weighted less in M_z ($M_{z,th}$ = 112k, M_z = 88k, Table S7†).

Finally, to demonstrate the mildness and versatility of photo-mediated RAFT step-growth polymerization, we prepared graft copolymers with a photodegradable backbone. Under the same reaction conditions as above, disulfide bond tethered bifunctional CTA (CTA_{2SS}) was polymerized with M_2 *via* PET-RAFT using red light (Fig. 3A, Table S8 and Fig. S12†). Remarkably, despite having relatively labile disulfide bonds in each repeat unit, the polymerization proceeded to follow step-growth molecular weight evolution as expected (Fig. S13†). In addition, structural analysis by ^{1}H-NMR spectroscopy was consistent with the intact backbone (Fig. S14†). Unexpectedly, we encountered some difficulty in removing the photocatalyst by precipitation of the polymer from diethyl ether. We have made some attempts to purify the polymer further by passing through aluminium oxide; though there were some visible differences, the presence of the catalyst was still noticeable (Fig. S15†). Nonetheless, we employed this backbone to graft poly(butylacrylate) (PBA) *via* RAFT-iniferter using the same photoreactor with blue light (Fig. S16†). We obtained 40% conversion after 2 hours, using a monomer to CTA ratio of 40 ($[BA]_0/[CTA]_0$ = 40) in dioxane ($[M]_0$ = 3 M), which yielded M_n

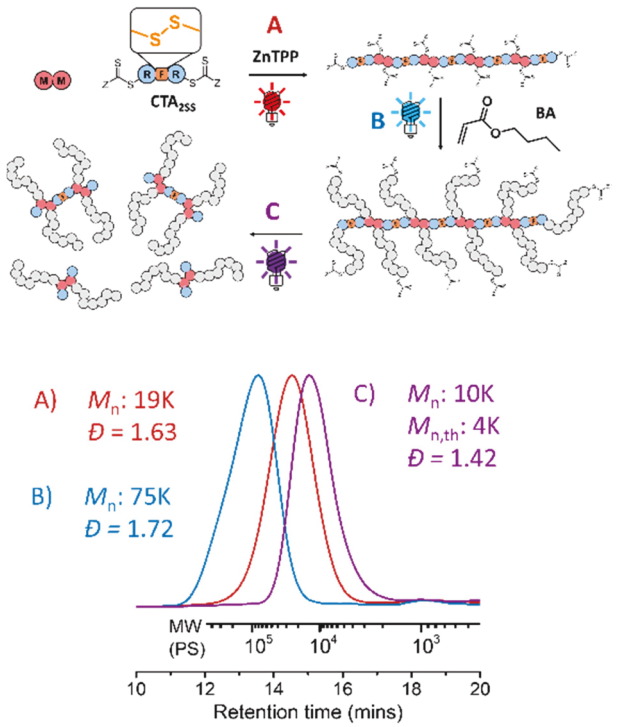

Fig. 3 (A) PET-RAFT step-growth polymerization with disulfide-tethered bifunctional CTA_2 using red light. (B) Grafting PBA from the resulting step-growth backbone *via* RAFT-iniferter using blue light. (C) Photocleavage of the backbone under ultraviolet light.

of approximately 2k per PBA side chain (Fig. S16†). Moreover, SEC analysis reveals a shift in molecular weight distribution whilst maintaining a unimodal shape, indicating a fully intact backbone (Fig. 3B and Fig. S17†). This is rather remarkable, given that disulfide bonds are classically known to undergo homolytic fission under irradiation with ultraviolet light.[33] We emphasize the mildness of both PET-RAFT and RAFT-iniferter using visible light, which permits the incorporation of a relatively photolabile functional group into the core of a complex structure. Indeed, subjecting the graft copolymer to ultraviolet irradiation results in the partial cleavage of the graft copolymer backbone (Fig. 3C; see Fig. S18† for the complete cleavage of the backbone using a reducing agent).

In summary, photo-mediated RAFT step-growth polymerization with maleimide monomers was demonstrated for the first time. The polymerization can be conducted under catalyst-free conditions at appreciable rates with green and blue light, whilst longer wavelengths (red light) can be employed in the presence of ZnTPP. The initial rates were comparably faster with green and blue light under catalyst-free conditions; however, the rate was found to plateau with increasing conversions, deviating from first-order kinetics. In contrast, the rate did not deviate significantly from the first order kinetics in the presence of the photocatalyst. Furthermore, the mildness and versatility of this approach were demonstrated by incorporating photolabile disulfide bonds in the step-growth polymer backbone and grafting polymeric side chains with light. It is worth noting that post polymerization modification is typically required for preparing graft copolymers when using the same polymerization (*e.g.*, RAFT chain-growth) for the side chains as for the main chain;[32] here, we use the step-growth CTA backbone to directly graft from *via* RAFT chain-growth polymerization without any additional step in between, thus greatly simplifying the preparation of such complex polymers.

Author contributions

The manuscript was written through the contributions of all authors.

Conflicts of interest

The authors declare the following competing financial interest (s): J. T. and W. Y. are named inventors on the provisional patent application described in this work.

Acknowledgements

This work was financially supported by the National Science Foundation (NSF) under Award CHE-2108670. A Bruker AVANCE III Nanobay 400 MHz NMR spectrometer was supported by the National Science Foundation under Grant No. CHE-0922858. The authors thank Dr Marc A. ter Horst from the University of North Carolina's Department of Chemistry NMR Core Laboratory for the use of the NMR spectrometers.

References

1 J. Chiefari, Y. K. Chong, F. Ercole, J. Krstina, J. Jeffery, T. P. T. Le, R. T. A. Mayadunne, G. F. Meijs, C. L. Moad, G. Moad, E. Rizzardo and S. H. Thang, *Macromolecules*, 1998, **31**, 5559–5562.
2 N. Corrigan, K. Jung, G. Moad, C. J. Hawker, K. Matyjaszewski and C. Boyer, *Prog. Polym. Sci.*, 2020, **111**, 101311.
3 S. Perrier, *Macromolecules*, 2017, **50**, 7433–7447.
4 M. Hartlieb, *Macromol. Rapid Commun.*, 2022, **43**, 2100514.
5 J. Xu, S. Shanmugam, N. A. Corrigan and C. Boyer, in *Controlled Radical Polymerization: Mechanisms*, American Chemical Society, 2015, vol. 1187, ch. 13, pp. 247–267.
6 T. Otsu and M. Yoshida, *Rapid Commun.*, 1982, **3**, 127–132.
7 P. Delduc, C. Tailhan and S. Z. Zard, *J. Chem. Soc., Chem. Commun.*, 1988, 308–310, DOI: **10.1039/C39880000308**.
8 S. Shanmugam, J. Cuthbert, J. Flum, M. Fantin, C. Boyer, T. Kowalewski and K. Matyjaszewski, *Polym. Chem.*, 2019, **10**, 2477–2483.
9 S. Shanmugam, J. Cuthbert, T. Kowalewski, C. Boyer and K. Matyjaszewski, *Macromolecules*, 2018, **51**, 7776–7784.

10 T. G. McKenzie, Q. Fu, M. Uchiyama, K. Satoh, J. Xu, C. Boyer, M. Kamigaito and G. G. Qiao, *Adv. Sci.*, 2016, **3**, 1500394.
11 P. J. Flory, *J. Am. Chem. Soc.*, 1936, **58**, 1877–1885.
12 J. Xu, C. Fu, S. Shanmugam, C. J. Hawker, G. Moad and C. Boyer, *Angew. Chem., Int. Ed.*, 2017, **56**, 8376–8383.
13 N. Corrigan, D. Rosli, J. W. J. Jones, J. Xu and C. Boyer, *Macromolecules*, 2016, **49**, 6779–6789.
14 S. Shanmugam, J. Xu and C. Boyer, *J. Am. Chem. Soc.*, 2015, **137**, 9174–9185.
15 J. Xu, K. Jung, A. Atme, S. Shanmugam and C. Boyer, *J. Am. Chem. Soc.*, 2014, **136**, 5508–5519.
16 J. Tanaka, N. E. Archer, M. J. Grant and W. You, *J. Am. Chem. Soc.*, 2021, **143**, 15918–15923.
17 P. Boeck, N. Archer, J. Tanaka and W. You, *Polym. Chem.*, 2022, **13**, 2589–2594.
18 N. E. Archer, P. T. Boeck, Y. Ajirniar, J. Tanaka and W. You, *ACS Macro Lett.*, 2022, 1079–1084, DOI: **10.1021/acsmacrolett.2c00476**.
19 A. Bossion, K. V. Heifferon, L. Meabe, N. Zivic, D. Taton, J. L. Hedrick, T. E. Long and H. Sardon, *Prog. Polym. Sci.*, 2019, **90**, 164–210.
20 Z. Huang, N. Corrigan, S. Lin, C. Boyer and J. Xu, *J. Polym. Sci., Part A: Polym. Chem.*, 2019, **57**, 1947–1955.
21 K. Skrabania, A. Miasnikova, A. M. Bivigou-Koumba, D. Zehm and A. Laschewsky, *Polym. Chem.*, 2011, **2**, 2074–2083.
22 A. Aerts, R. W. Lewis, Y. Zhou, N. Malic, G. Moad and A. Postma, *Macromol. Rapid Commun.*, 2018, **39**, 1800240.
23 L. T. Strover, A. Cantalice, J. Y. L. Lam, A. Postma, O. E. Hutt, M. D. Horne and G. Moad, *ACS Macro Lett.*, 2019, **8**, 1316–1322.
24 Z. Li, J. Li, X. Pan, Z. Zhang and J. Zhu, *ACS Macro Lett.*, 2022, 230–235, DOI: **10.1021/acsmacrolett.1c00762**.
25 Y. Zhou, Z. Zhang, C. M. Reese, D. L. Patton, J. Xu, C. Boyer, A. Postma and G. Moad, *Macromol. Rapid Commun.*, 2020, **41**, 1900478.
26 P. Seal, J. Xu, S. De Luca, C. Boyer and S. C. Smith, *Adv. Theory Simul.*, 2019, **2**, 1900038.
27 R. N. Carmean, M. B. Sims, C. A. Figg, P. J. Hurst, J. P. Patterson and B. S. Sumerlin, *ACS Macro Lett.*, 2020, **9**, 613–618.
28 H. Wang, Q. Li, J. Dai, F. Du, H. Zheng and R. Bai, *Macromolecules*, 2013, **46**, 2576–2582.
29 C. A. Figg, J. D. Hickman, G. M. Scheutz, S. Shanmugam, R. N. Carmean, B. S. Tucker, C. Boyer and B. S. Sumerlin, *Macromolecules*, 2018, **51**, 1370–1376.
30 R. Liu, L. Zhang, Z. Huang and J. Xu, *Polym. Chem.*, 2020, **11**, 4557–4567.
31 H. R. Kricheldorf, *Macromol. Rapid Commun.*, 2007, **28**, 1839–1870.
32 A. Kerr, M. Hartlieb, J. Sanchis, T. Smith and S. Perrier, *Chem. Commun.*, 2017, **53**, 11901–11904.
33 E. E. Smissman and J. R. J. Sorenson, *J. Org. Chem.*, 1965, **30**, 4008–4010.